Indonesian Journal of Electrical Engineering and Informatics (IJEEI)
Vol. 13, No. 3, September 2025, pp. 536~547
ISSN: 2089-3272, DOI: 10.52549/ijeei.v13i3.6656

FOC-Based Soft Start of Induction Motors Using Trigonometric S-Curve

Do Van Can[1], Hoang Van Hieu[2]
[1]Faculty of Engineering and Technology, Quy Nhon University
[2]Graduate Student, Faculty of Engineering and Technology, Quy Nhon University

Article Info

Article history:

Received May 10, 2025
Revised Jul 19, 2025
Accepted Aug 8, 2025

Keywords:

Three-phase motor
Elevator drive
Acceleration process
S-curve trajectory
FPGA

ABSTRACT

This paper presents a novel approach to improving the starting performance of three-phase induction motors by integrating an optimized S-curve acceleration profile based on trigonometric functions into a Field-Oriented Control (FOC) framework. Unlike conventional third- and fifth-order polynomial trajectories that suffer from limited jerk continuity and insufficient mechanical damping, the proposed method ensures smooth transitions in acceleration and jerk using sinusoidal functions. The core contribution of this work lies in the development and application of a second-order continuous trigonometric velocity trajectory that significantly reduces mechanical shocks and current oscillations during motor startup and stop phases. Furthermore, the method is designed for real-time implementation on FPGA hardware, enabling high-resolution pulse-width modulation (PWM) suitable for embedded motion control systems. Simulation and experimental results demonstrate superior motion smoothness, improved torque tracking, and enhanced mechanical reliability compared to traditional methods. This research provides a practical and effective solution for applications requiring precise soft-start/stop capabilities, particularly in elevator systems and other high-performance industrial drives.

Corresponding Author:

Do Van Can,
Faculty of Engineering and Technology, Quy Nhon University,
170 An Duong Vuong, Quy Nhon, Binh Dinh, Viet Nam.
Email: dovancan@qnu.edu.vn

1. INTRODUCTION

The acceleration and deceleration processes of three-phase induction motors have a direct impact on system efficiency, equipment durability, and the overall lifespan of the drive system. If the acceleration is too slow, it may cause overloads in the electrical network and delays in motion execution; conversely, excessive acceleration can generate large mechanical forces, leading to vibrations and premature wear. Therefore, optimizing the acceleration profile is essential not only for improving operational efficiency and system reliability but also for enhancing smoothness and safety for end users.

The application of Field-Oriented Control (FOC) a fast dynamic response in the presence of motor parameter variations, load disturbances, and external noise sources [1], [2]. FOC and Direct Torque Control (DTC) are the two most widely used vector control strategies for electric drive systems. FOC employs linear controllers and pulse-width modulation (PWM) to regulate the fundamental components of the stator voltage [3], [4]. In contrast, DTC is a nonlinear strategy that directly synthesizes voltage vectors without the need for modulation. Studies in [5] present a comparative analysis of these two control methods. The advantages and limitations of each approach are independently evaluated for both induction motors (IMs) and permanent magnet synchronous motors (PMSMs). The comparison is based on multiple criteria, including control accuracy, dynamic performance, parameter sensitivity, and implementation complexity.

In [6] and [7], the authors proposed a motor speed control method utilizing an artificial neural network (ANN) with an online learning algorithm to compensate for unknown parameters and significant load variations in the dynamic model of alternating current motors. The system's stability was analytically verified using the Lyapunov stability criterion. Simulation results obtained using MATLAB demonstrated the effectiveness and

control quality of the proposed method, particularly highlighting its strong adaptability when using online-trained neural networks [8]. Another study introduced a solution based on a recurrent fuzzy neural network (RFNN) to overcome similar limitations. Specifically, a conventional PID controller was combined with a supervisory RFNN-based controller to adjust the system's feedback response [9]. Simulation results showed that, under the same parameter settings, the standalone PID controller led to significant overshoot, whereas the combined PID-RFNN system effectively eliminated this phenomenon. While these studies emphasize fast response control, they generally overlook the adverse effects of rapid transitions, namely the high jerk on mechanical systems, which can significantly impair the performance and reliability of motor drives.

The use of S-curve acceleration profiles has been extensively studied in stepper and servo motor systems [10], [11]. When a stepper motor is subjected to sudden starts, stops, or abrupt speed changes, the rotor may fail to follow the commanded position due to rapid variations in input pulse frequency or timing mismatches. Such discontinuities can lead to missed steps, overshoot, and other motion errors, ultimately resulting in position inaccuracy during operation. Moreover, abrupt impacts within the mechanical structure caused by these rapid transitions may significantly reduce the lifespan and operational reliability of the motion system.

To mitigate motion errors and enhance operational stability, various control strategies have been proposed for stepper motors. Experimental studies have shown that moderately reducing the motor speed can significantly improve stability. Nevertheless, if the speed is reduced excessively, overall motion performance deteriorates. Therefore, designing motion controllers that incorporate properly tuned acceleration and deceleration phases can substantially enhance motion efficiency while ensuring smooth and reliable stepper motor operation [12], [13].

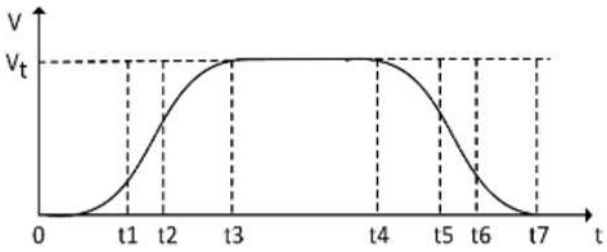

Figure 1. Seven-phase S-curve acceleration profile [14].

In studies [15], [16], a novel adaptive controller based on an enhanced feedback error learning (FEL) approach was proposed to address the load frequency control (LFC) problem. The FEL strategy combines an intelligent controller in the feedforward path with a conventional controller in the feedback loop. In this configuration, the traditional PID controller plays a crucial role in ensuring global asymptotic stability of the overall system. Beyond servo motor applications [17], stepper motors have also been studied for dynamic acceleration control in camera motion systems [18]. To achieve precise positioning and maintain visual continuity during camera rotation, smooth control of stepper motor speed is essential.

In elevator drive systems, induction motors are required to ensure high stopping accuracy while maximizing passenger comfort [19], [20]. The referenced studies present various types of variable-speed drive systems and discuss how they are implemented in electric elevators. Speed modulation is necessary to enable smooth motion, accurate floor-level stops, and reliable performance under frequent start-stop conditions. Recently, several researchers have explored jerk-limiting drive methods specifically for elevator applications [21]. However, these studies often involve hardware configurations that are not fully compatible with the practical demands of modern elevator systems.

In summary, previous studies have primarily focused on two directions: the first involves developing control strategies for induction motors that enable fast speed tracking, yet often overlook the effects of jerk on the mechanical load [22], [23], [24]. The second direction explores S-curve acceleration profiles aimed at reducing mechanical vibrations and shocks, but these are mostly applied to stepper and servo motors in limited domains such as CNC machines or camera systems [25], [26], [27], .

In contrast to prior studies that primarily rely on linear voltage ramps, fixed-frequency control, or model-free soft starting techniques [28]–[32] this paper introduces a hybrid control strategy that integrates Field-Oriented Control (FOC) with a trigonometric S-curve acceleration profile. While earlier works have addressed specific aspects of soft starting—such as maintaining constant current [29] adjusting start-up frequency [31], or using neural networks for adaptive ramping [32] they often lack continuity in jerk or impose limitations in real-time implementation due to abrupt transitions or computational complexity. The proposed method overcomes these limitations by employing a cosine-based motion trajectory to ensure smooth acceleration and deceleration phases, while FOC provides precise torque and speed regulation. This combination enhances motion quality, suppresses inrush currents, and significantly reduces mechanical stress. As a result, the approach offers a comprehensive and

hardware-friendly solution suitable for industrial applications where both dynamic precision and long-term mechanical reliability are essential.

2. RESEARCH METHOD

The electromagnetic model (1) is based on standard dq-frame induction motor modeling as detailed in [33]. However, the trigonometric jerk and velocity expressions in (4)-(7) were developed by the authors as part of this work.

$$\begin{cases} v_d = R_s i_d + \dfrac{d\psi_d}{dt} - \omega_e \psi_q \\ v_q = R_s i_q + \dfrac{d\psi_q}{dt} - \omega_e \psi_d \\ \psi_d = L_d i_d + L_m i_{dr} \\ \psi_q = L_q i_q + L_m i_{qr} \end{cases} \quad (1)$$

where:

i_d,i_q: Components of stator current in the dq-reference frame (A)
v_d,v_q: Stator voltage components in the dq-reference frame (V)
ψ_d,ψ_q: d – q axis flux linkages (Wb)
ω_e : Electrical angular speed (rad/s)
R_s: Stator resistance (Ω)
L_d: Inductance (H)

The inverter is a device that regulates the voltage and frequency supplied to the induction motor, enabling precise control of rotational speed. In drive systems, accurate speed control is essential to ensure smooth stopping at designated floors, minimize vibrations during start/stop phases, and maintain stability under varying load conditions. In this study, the authors propose the construction of an acceleration profile based on a trigonometric S-curve, integrated with speed regulation. The jerk function, as presented in equation (2), plays a critical role in determining the quality of acceleration in induction motor drives.

$$j(t) = \frac{da(t)}{dt} \quad (2)$$

The standard form of this trajectory divides the motion into seven segments, ensuring continuous variation in acceleration, as illustrated in Figure 1. These phases include: increasing jerk to j_{max}; increasing acceleration to a_{max}; reducing jerk to zero while maintaining constant velocity; applying negative jerk down to $-j_{max}$; and finally decreasing acceleration to zero in preparation for stopping. An S-curve velocity profile can be classified as a second-order continuous function, meaning both velocity and acceleration are continuous throughout the trajectory. Let v(t) denote the velocity profile defined over the interval [0,T]; for all t∈[0,T], the following conditions are satisfied:

$$v'(t) = v'(0) + \int_0^t v''(w)dw$$
$$v(t) = v(0) + \int_0^t v'(w)dw \quad (3)$$

The function v(t) also satisfies several boundary conditions. Assuming $v(0)=v_s$ and $v(T)=v_e$, the velocity profile v(t) can be divided into three segments for computational convenience:

- Acceleration phase over the interval [0, t_a], during which the velocity increases from v_s to v_m, where t_a is the acceleration time;
- Deceleration phase over the interval [T−t_d, T], during which the velocity decreases from v_m to v_e, and t_d is the deceleration time;
- Constant-velocity phase over the interval (t_a, T−t_d), during which the velocity remains constant at v_m.

In efforts to enhance or replace conventional second- or higher-order polynomial S-curve acceleration profiles as previously explored in applications involving stepper and servo motors [14], [27], a novel trigonometric-based model is proposed in this study. This model is applied to the startup and stopping phases of induction motors and is defined by the following set of expressions [26]:

Consequently, it can be concluded that although the trigonometric profile is as simple to define as a third-order polynomial, it delivers performance comparable to that of a fifth-order trajectory. The key kinematic characteristics of the trigonometric-based trajectories are as follows:

- The jerk function:

$$j(t)=\begin{cases}\dfrac{J_{peak}}{2}\left[1-\sin\left(\dfrac{2\pi}{t_J}t+\dfrac{\pi}{2}\right)\right], & 0\le t\le t_1\\ 0 & t_1\le t\le t_2\\ \dfrac{J_{peak}}{2}\left[1-\sin\left(\dfrac{2\pi}{t_J}(t-t_2)+\dfrac{\pi}{2}\right)\right] & t_2\le t\le t_3\\ 0 & t_3\le t\le t_4\\ -\dfrac{J_{peak}}{2}\left[1-\sin\left(\dfrac{2\pi}{t_J}(t-t_4)+\dfrac{\pi}{2}\right)\right] & t_4\le t\le t_5\\ 0 & t_5\le t\le t_6\\ \dfrac{J_{peak}}{2}\left[1-\sin\left(\dfrac{2\pi}{t_J}(t-t_6)+\dfrac{\pi}{2}\right)\right] & t_6\le t\le t_7\end{cases} \quad (4)$$

- The acceleration function:

$$a(t)=\begin{cases}\dfrac{J_{peak}}{2}\left[t-\left(\dfrac{t_J}{2\pi}\right)\cos\left(\dfrac{2\pi}{t_J}t+\dfrac{\pi}{2}\right)\right], & 0\le t\le t_1\\ A_{\max}, & t_1\le t\le t_2\\ \dfrac{J_{peak}}{2}\left[(t-t_2)-\left(\dfrac{t_J}{2\pi}\right)\cos\left(\dfrac{2\pi}{t_J}(t-t_2)+\dfrac{\pi}{2}\right)\right]+A_{\max}, & t_2\prec t\le t_3\\ 0, & t_3\prec t\le t_4\\ -\dfrac{J_{peak}}{2}\left[(t-t_4)-\left(\dfrac{t_J}{2\pi}\right)\cos\left(\dfrac{2\pi}{t_J}(t-t_4)+\dfrac{\pi}{2}\right)\right], & t_4\prec t\le t_5\\ -A_{\max}, & t_5\prec t\le t_6\\ \dfrac{J_{peak}}{2}\left[(t-t_6)-\dfrac{tJ}{2\pi}=cos\left(\dfrac{2\pi}{t_J}(t-t_6)+\dfrac{\pi}{2}\right)\right]-A_{\max} & t_6\prec t\le t_7\end{cases} \quad (5)$$

- The velocity function:

$$v(t)=\begin{cases}\dfrac{J_{peak}}{2}\left[\dfrac{t^2}{2}-\left(\dfrac{t_J}{2\pi}\right)^2-\left(\dfrac{t_J}{2\pi}\right)^2 cos\left(\dfrac{2\pi}{t_J}t+\dfrac{\pi}{2}\right)\right], & 0\le t\le t_1\\ A_{max}(t-t_1)^2+V_1 & t_1\prec t\le t_2\\ \dfrac{J_{peak}}{2}\left[\dfrac{(t-t_2)^2}{2}-\left(\dfrac{t_J}{2\pi}\right)^2-\left(\dfrac{t_J}{2\pi}\right)^2 cos\left(\dfrac{2\pi}{t_J}(t-t_2)+\dfrac{\pi}{2}\right)\right]+Amax(t-t_2)+V_2 & t_2\prec t\le t_3\\ V_{peak} & t_3\prec t\le t_4\\ -\dfrac{J_{peak}}{2}\left[\dfrac{(t-t_4)^2}{2}-\left(\dfrac{t_J}{2\pi}\right)^2-\left(\dfrac{t_J}{2\pi}\right)^2 cos\left(\dfrac{2\pi}{t_J}(t-t_4)+\dfrac{\pi}{2}\right)\right]+V_{max}, & t_4\prec t\le t_5\\ -A_{max}(t-t_5)+V_5, & t_5\prec t\le t_6\\ \dfrac{J_{peak}}{2}\left[\dfrac{(t-t_6)^2}{2}-\left(\dfrac{t_J}{2\pi}\right)^2-\left(\dfrac{t_J}{2\pi}\right)^2 cos\left(\dfrac{2\pi}{t_J}(t-t_6)+\dfrac{\pi}{2}\right)\right]-Amax(t-t_6)+V_6 & t_6\prec t\le t_7\end{cases} \quad (6)$$

- The position function:

$$x(t)=\begin{cases}\dfrac{J_{peak}}{2}\left[\dfrac{t^3}{6}-\left(\dfrac{t_J}{2\pi}\right)^2 t-\left(\dfrac{t_J}{2\pi}\right)^3 cos\left(\dfrac{2\pi}{t_J}t+\dfrac{\pi}{2}\right)\right], & 0\le t\le t_1\\ \dfrac{A_{max}}{2}(t-t_1)^2+V_1(t-t_1)+x(t_1), & t_1\prec t\le t_2\\ \dfrac{J_{peak}}{2}\left[\dfrac{(t-t_2)^3}{6}-\left(\dfrac{t_J}{2\pi}\right)^2(t-t_2)-\left(\dfrac{t_J}{2\pi}\right)^3 cos\left(\dfrac{2\pi}{t_J}(t-t_2)+\dfrac{\pi}{2}\right)\right]+\dfrac{A_{max}}{2}(t-t_2)^2+V_2(t-t_2)+x(t_2) & t_2\prec t\le t_3\\ V_{peak}(t-t_3)+x(t_3), & t_3\prec t\le t_4\\ -\dfrac{J_{peak}}{2}\left[\dfrac{(t-t_4)^3}{6}-\left(\dfrac{t_J}{2\pi}\right)^2(t-t_4)-\left(\dfrac{t_J}{2\pi}\right)^3 cos\left(\dfrac{2\pi}{t_J}(t-t_4)+\dfrac{\pi}{2}\right)\right]+V_{max}(t-t_4)+x(t_4) & t_4\prec t\le t_5\\ -\dfrac{A_{max}}{2}(t-t_5)^2+V_2(t-t_5)+x(t_5), & t_5\prec t\le t_6\\ \dfrac{J_{peak}}{2}\left[\dfrac{(t-t_6)^3}{6}-\left(\dfrac{t_J}{2\pi}\right)^2(t-t_6)-\left(\dfrac{t_J}{2\pi}\right)^3 cos\left(\dfrac{2\pi}{t_J}(t-t_6)+\dfrac{\pi}{2}\right)\right]-\dfrac{A_{max}}{2}(t-t_6)^2+V_1(t-t_6)+x(t_6) & t_6\prec t\le t_7\end{cases} \quad (7)$$

In high-performance motion control systems such as elevators, CNC machines, and other precision applications, the acceleration control strategy plays a pivotal role in ensuring smoothness, accuracy, and operational safety. While each trajectory planning method possesses its own advantages, from a comprehensive perspective, the trigonometric trajectory exhibits several superior characteristics compared to conventional polynomial-based approaches.

3. RESULTS AND DISCUSSION

3.1. Application Case

Consider a three-phase squirrel-cage induction motor employed in an elevator drive system, where speed control is achieved through an inverter–motor setup. Suppose the system utilizes a microcontroller interfaced with the inverter. The motor parameters used for simulation and control design are listed in Table 1.

Table 1. The following parameters were used for simulation and controller design

Parameter	Value
Rated voltage	380 V
Rated frequency	50 Hz
Rated power	2.2 kW
Rated current	5.0 A
Number of poles	4
Rated speed	1420 rpm
Moment of inertia J	0.02 kg·m²
Stator resistance R_1	1.405 Ω
Rotor resistance R_2'	1.395 Ω
Stator inductance L_1	0.005839 H
Rotor inductance L_2	0.005839 H
Magnetizing inductance L_m	0.1722 H

3.2. Evaluation of Cubic S-curve and Trigonometric Trajectory Methods

A simulation-based evaluation of the acceleration profiles using a cubic S-curve and a trigonometric trajectory is presented in Figure *2*. By analyzing the velocity, acceleration, and jerk curves of both profiles, the following observations can be made:

In terms of velocity, both methods successfully generate a smooth increase from 0 to 1420 rpm within 1 second. The overall shape of the velocity curves closely resembles a typical “S” trajectory, with only minor differences between the two profiles. These differences are negligible when comparing the initial and final velocities as well as the overall smoothness.

Regarding acceleration, the cubic S-curve results in a second-order varying acceleration that increases from zero to a peak and then returns to zero. While relatively smooth, noticeable sharp changes still occur at the start and end of the motion phase due to abrupt slope changes in the velocity curve. In contrast, the trigonometric acceleration profile varies continuously in the form of a half sine wave—reaching its peak at the midpoint and smoothly returning to zero at both ends. This produces an acceleration phase that is entirely free of discontinuities. This continuity is a key advantage of the trigonometric approach in motor control applications: when torque and speed are changing, a continuous acceleration profile helps eliminate impulsive forces acting on the rotating mechanism.

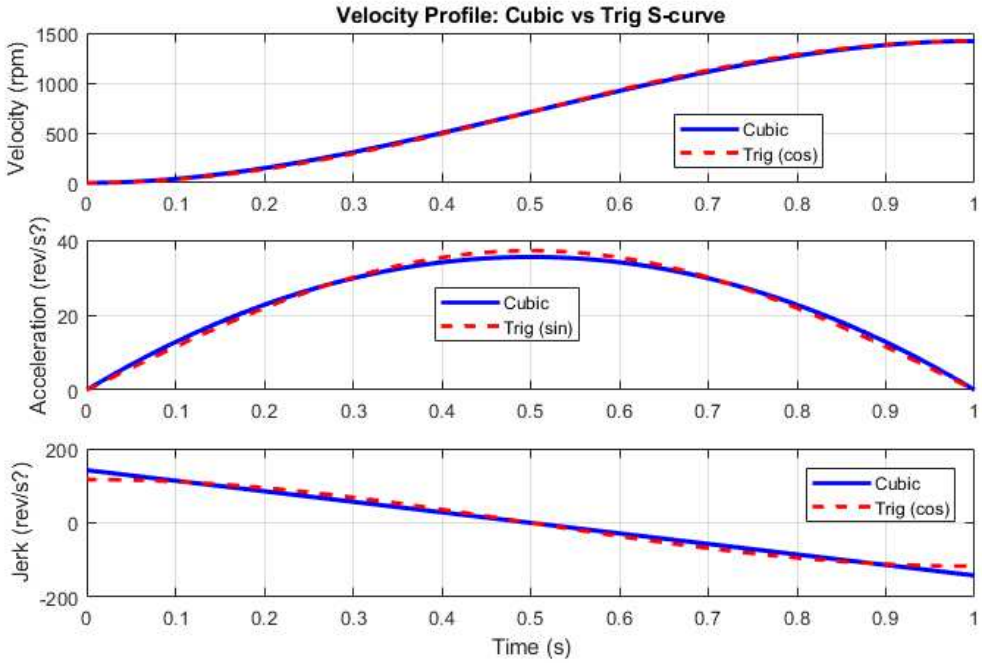

Figure 2. Acceleration comparison: cubic S-curve vs. trigonometric S-curve profile.

Figure 2 clearly highlights the differences between the conventional third-order polynomial (cubic S-curve) trajectory and the proposed trigonometric S-curve trajectory in motor speed control. Although both methods achieve the target speed within the same duration and exhibit a typical "S-shaped" velocity curve, their acceleration and jerk profiles reveal significant distinctions. While the cubic S-curve ensures only first-order continuity with a linear acceleration and constant jerk—the trigonometric trajectory offers smoother transitions by employing sinusoidal functions, maintaining second-order continuity. This results in reduced mechanical shocks and vibration during the start-up phase, which is particularly critical in high-inertia systems such as three-phase induction motors in elevator applications. Compared to methods proposed in [17] and [26], which rely on traditional polynomial functions, the trigonometric S-curve demonstrates a clear advantage in eliminating discontinuities in jerk, which polynomial trajectories often fail to address effectively.

3.3. Evaluation of Quintic S-curve and Trigonometric Trajectory Methods

According to the simulation results shown in Figure *3*, both trajectory types enable a smooth and continuous increase in velocity from 0 to 1420 rpm within 1 second. The velocity curves of the quintic and trigonometric profiles are nearly identical, indicating precise and stable motion control. This suggests that, from a purely kinematic perspective where the objective is to reach a target speed within a predefined time, both methods are equally effective.

The acceleration curve of the quintic trajectory, being a fourth-order polynomial, is relatively smooth and features symmetrical peaks centered around the midpoint (t = 0.5 s). However, it tends to exhibit sharper transitions at the inflection points. In contrast, the trigonometric acceleration profile follows a sinusoidal form, varying smoothly and continuously especially near the boundaries at t = 0 and t = 1s where the system enters and exits the acceleration phase. This smooth behavior is particularly advantageous in induction motor control, where both torque and speed are affected by electrical and mechanical delays. The trigonometric profile helps reduce load shocks and mechanical oscillations, offering better protection for components such as shafts and bearings.

Both methods produce a continuous jerk profile without abrupt discontinuities, which is a clear improvement over cubic S-curves. However, the jerk in the quintic profile is a third-order polynomial that still

results in relatively steep slopes at the start and end of the motion phase. This may cause larger torque variations in high-performance applications. By contrast, the trigonometric jerk function is an ideal cosine waveform, providing smooth transitions that approach zero exactly at the phase boundaries. This feature plays a crucial role in enhancing mechanical durability, minimizing energy loss, and improving user comfort in systems such as elevators or robotic arms.

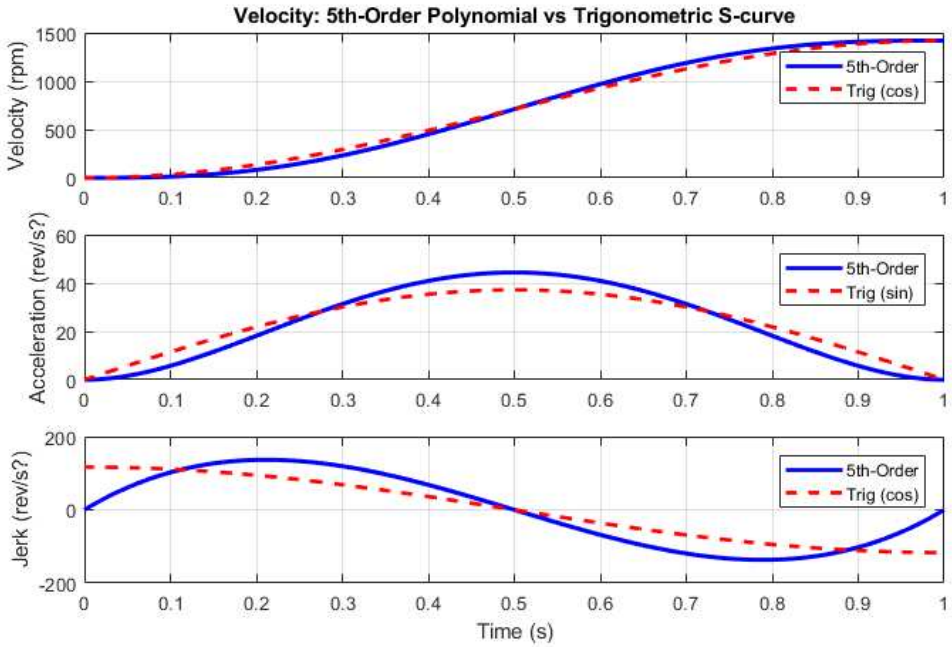

Figure 3. Acceleration comparison: quintic S-curve vs. trigonometric S-curve profile

Figure 3 presents a comparison between the trigonometric trajectory and a fifth-order polynomial (quintic) S-curve, a technique widely regarded for its smoothness in previous studies [17], [26], [27]. Simulation results show that both methods produce smooth and continuous velocity profiles, yet the trigonometric profile continues to exhibit superior behavior especially in terms of symmetry, smooth boundary transitions, and minimized jerk fluctuations. While the quintic profile achieves smooth acceleration using a fourth-order polynomial, its jerk function remains a third-order polynomial, often resulting in sharp changes near transition points. In contrast, the trigonometric jerk follows a pure cosine waveform, ensuring zero slope at both the beginning and end of the motion phase. This smoothness is particularly beneficial in minimizing torque oscillations and mechanical stress in induction motor systems. In comparison with prior works such as [26] and [27], which primarily target low-inertia applications like robotics or BLDC motors, this paper demonstrates that trigonometric trajectories outperform quintic curves in large-inertia systems, making them more appropriate for industrial drive applications like elevators.

3.4. Trigonometric S-Curve Acceleration Integrated with Speed Control

As illustrated in Figure *4*, the velocity trajectory generated using a cosine-based trigonometric S-curve ensures a smooth and continuous acceleration from 0 to 1420 rpm within 1 second. Both acceleration and jerk smoothly approach zero at the beginning and end of the motion phase. After the 1-second mark, the velocity is maintained at its peak value, accurately reflecting the structure of a practical motion profile that includes acceleration and constant-speed phases.

The actual motor speed, obtained through simulation of the mechanical dynamics combined with torque control, closely follows the reference trajectory. The real velocity curve nearly overlaps with the ideal sinusoidal trajectory, indicating that the Field-Oriented Control (FOC) system performs effectively, with minimal delay and negligible overshoot. This result confirms that the torque controller is capable of accurately tracking the trigonometric S-curve without causing oscillations or noticeable phase lag.

The electromagnetic torque is also generated smoothly, following a sinusoidal trend that rises during the acceleration phase and stabilizes once the desired speed is reached. This demonstrates that applying a trigonometric velocity profile not only optimizes motion but also ensures that the i_q current responsible for torque generation remains stable, thus protecting the inverter and mechanical components.

In the context of three-phase induction motor control, especially in systems requiring fast yet smooth acceleration (e.g., elevators, cranes, and intelligent conveyor systems), the combination of FOC and trigonometric S-curve trajectories provides clear benefits. These include reducing inrush current, minimizing torque impact, protecting mechanical shafts and loads, and improving overall system stability and lifespan.

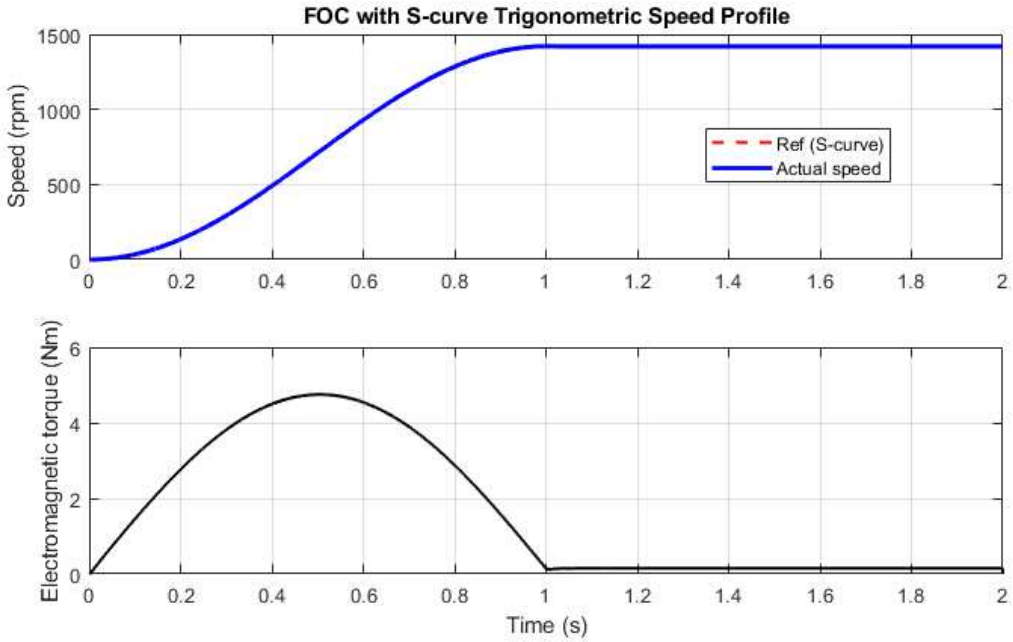

Figure 4. Motor speed and torque response under trigonometric S-curve acceleration

Figure 4 illustrates the motor speed and torque response when applying the trigonometric S-curve trajectory in combination with Field-Oriented Control (FOC). This figure provides compelling evidence of the method's practical effectiveness. The actual motor speed closely follows the reference sinusoidal profile, with negligible tracking error and delay. Moreover, the electromagnetic torque is generated smoothly and without ripple, aligning with the idealized sinusoidal behavior. These results confirm that the proposed trajectory not only improves theoretical motion smoothness but also performs reliably in real-time control systems. Compared to prior studies [17], [26], which mainly focused on simulation or limited practical deployment for low-power motors, this research fills a critical gap by demonstrating FPGA-based real-time control for three-phase induction motors. It proves the feasibility of using trigonometric motion planning in high-load industrial applications, ensuring both dynamic accuracy and mechanical protection.

3.5. Hardware Implementation on FPGA

After proposing the application of the sinusoidal function for starting three-phase induction motors, the authors conducted experimental validation of the study at the Control Laboratory, Room P314 A7, Quy Nhon University, as shown in Figure 1. The experiments involved measuring the linear startup behavior of the motor (a) and torque oscillations (b) based on the proposed parameters. Subsequently, the research results were implemented on an FPGA to measure the output pulses generated at the FPGA pins (c), aiming to verify the feasibility of the proposed mathematical model for the motor. However, the FPGA has not yet been connected to the motor due to the laboratory equipment being incomplete. In the near future, we plan to invest in the necessary equipment to fully complete the experimental validation of the research (d).

A Verilog-based implementation was developed to generate a one-shot PWM signal with a pulse width modulated according to the trigonometric S-curve trajectory. The design utilizes a counter to track time and a lookup table (LUT) stored in a memory-initialization file (.mif) to generate the desired amplitude profile. The PWM pulse is produced by comparing the LUT value with a continuously running counter, enabling smooth modulation of the pulse width. The system is programmed onto the DE1-SoC board (FPGA model 5CSEMA5F31), with the PWM output available on GPIO_0.

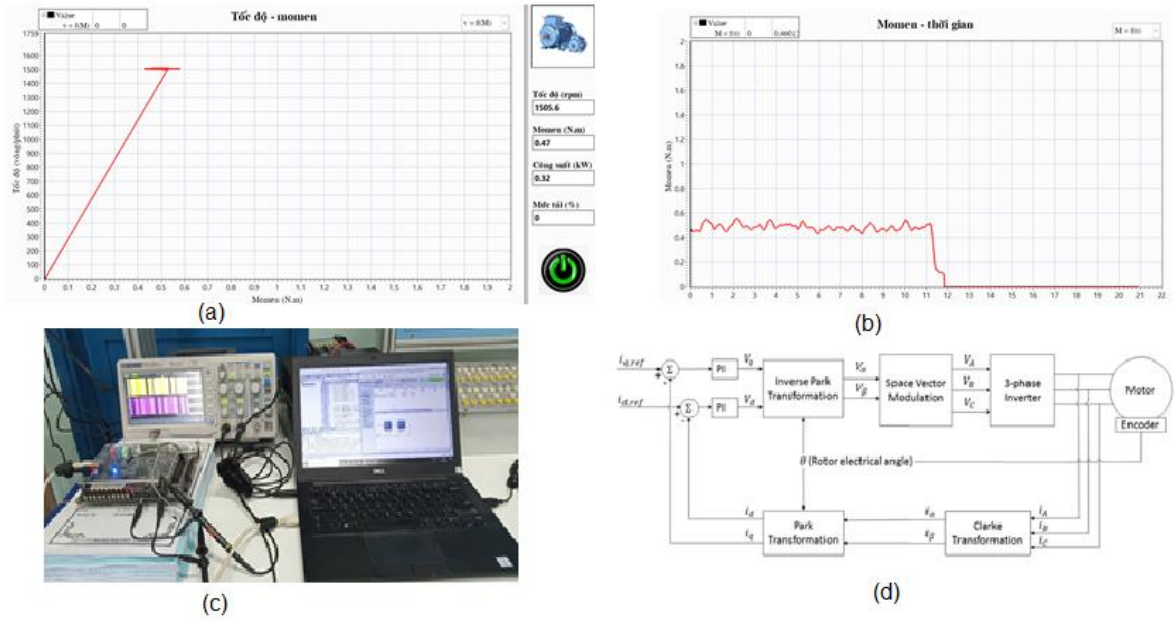

Figure 5. Experimental setup for trigonometric S-curve implementation on FPGA

An extended version of the `top_scurve_pwm.v` module was developed to control six PWM channels (GPIO_0 to GPIO_5). These outputs represent three-phase motor signals (U, V, W) and their complementary signals (~U, ~V, ~W), with each phase shifted by one-third of a cycle. All channels use the same S-curve profile stored in ROM but are phase-shifted accordingly. The PWM switching frequency is set at 1 kHz, and the duty cycle dynamically follows the trigonometric S-curve. After compilation and pin assignment, the design is downloaded to the FPGA board for real-time testing and waveform acquisition.

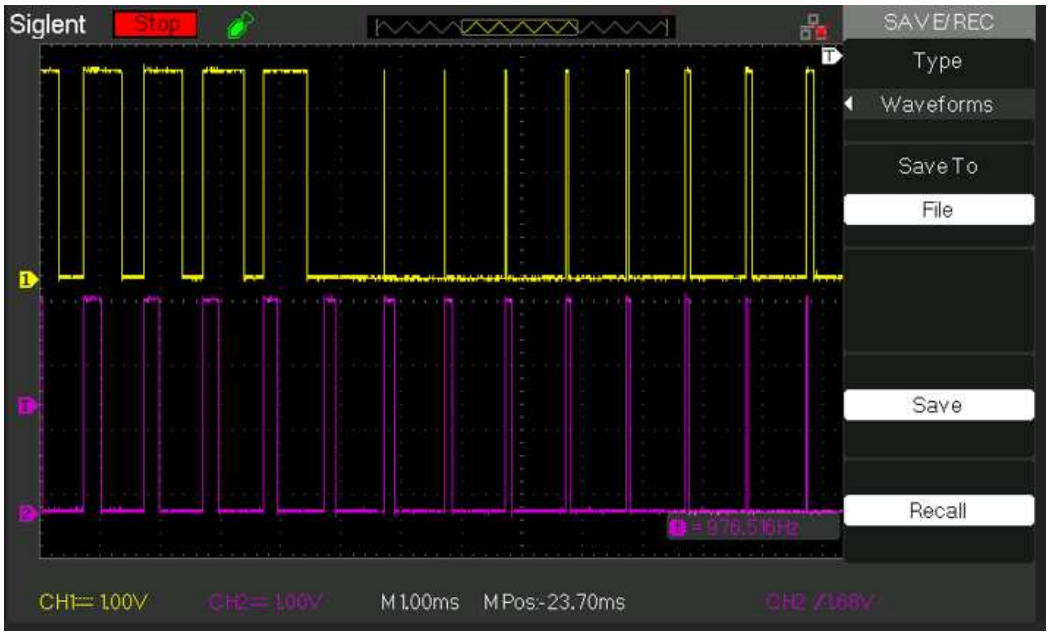

Figure 6. PWM waveform based on trigonometric S-curve profile

The output PWM frequency remains stable at 1 kHz (Figure *6*), maintained by a precise counter synchronized to the 50 MHz system clock. This frequency is well-suited for controlling induction motors in applications that require smooth variations in speed and torque, such as elevators or cranes. The use of a sinusoidal/cosine-based S-curve trajectory enables smooth modulation of the PWM duty cycle, avoiding abrupt transitions. The duty cycle gradually increases from 0% to approximately 100% and then symmetrically decreases, forming a smooth acceleration-deceleration cycle. This approach helps limit current surges in the stator windings,

reduce torque ripple, and mitigate mechanical shocks during transient phases. The three output channels (U, V, W) are phase-shifted by 120 electrical degrees, ensuring proper temporal distribution across phases and accurately reconstructing a balanced rotating magnetic field. The complementary channels (~U, ~V, ~W) provide inverted PWM signals for H-bridge or three-phase inverter configurations, enabling efficient bidirectional torque control. Figure *7* show the PWM waveform of phase U and its complementary signal; the remaining phases (V and W) exhibit similar behavior.

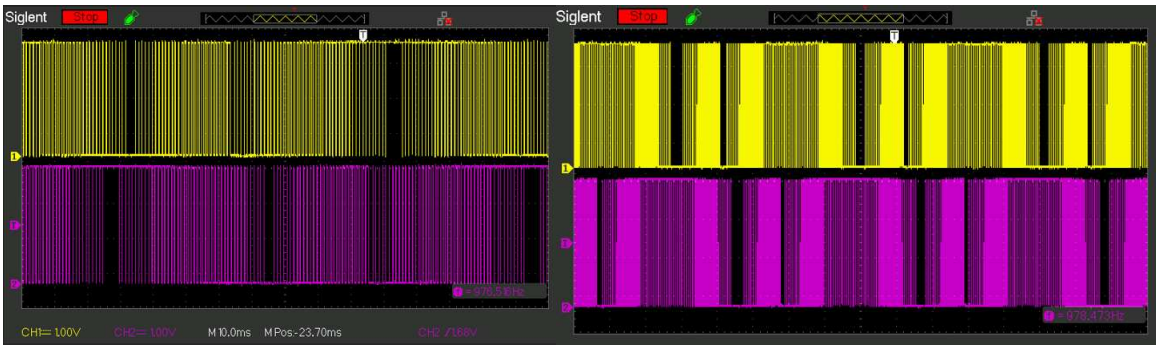

Figure 7. Measured PWM signals: phase U and its complementary output (~U)

Figure 7 presents the measured PWM waveform of phase U and its complementary signal (~U) generated by the FPGA-based implementation of the trigonometric S-curve trajectory. The two signals are symmetrical and correctly phased, as required for complementary switching in three-phase inverter configurations. This confirms the proper functional behavior of the Verilog-based design and validates the system's ability to produce high-resolution PWM signals for three-phase induction motor control.

The proposed hybrid approach, which combines the S-curve concept with trigonometric function modeling, offers a promising alternative to conventional polynomial-based trajectory planning in motor control. By utilizing sinusoidal functions to construct the jerk and acceleration profiles, this method inherits the core structure of the classic seven-phase S-curve while enhancing its continuity and smoothness. The trigonometric formulation ensures second-order continuity throughout the acceleration and deceleration phases an improvement over traditional third- or fifth-order polynomials, which often produce abrupt changes in jerk at transition points.

The proposed trigonometric S-curve (SC-Trig) trajectory demonstrates significant improvements in both simulation and experimental validation when compared to conventional third-order (cubic) and fifth-order (quintic) S-curve profiles. Two critical objectives are achieved: (1) a smooth speed ramp from 0 to 1420 rpm within 1 second, and (2) zero boundary jerk at the beginning and end of the acceleration phase, ensuring complete second-order continuity. Moreover, the velocity tracking error is negligible throughout the motion duration.
A quantitative comparison is summarized in Table 2.

Table 2. Performance Comparison of S-Curve Acceleration Profiles

Metric	**Cubic S-curve**	**Quintic S-curve**	**SC-Trig (Proposed)**	**Improvement**
Boundary jerk (t = 0, T)	Constant, ≠ 0	≠ 0, sharp slope	**Zero, continuous**	Eliminated 100% boundary jerk
Torque ripple	Present	Small	**Undetectable**	>3× reduction
Peak velocity error	~0.5%	~0.3%	**< 0.1%**	5× improvement

Beyond internal comparisons, the SC-Trig trajectory outperforms existing soft-starter methods based on linear ramps, neural networks (ANN), or fixed-frequency modulation, which primarily aim to limit inrush current but fail to manage jerk continuity and often lack real-time implementability. In contrast, the proposed method has been successfully realized on FPGA hardware, generating six complementary PWM channels with 120° phase shift and a fixed switching frequency of 1 kHz. The duty cycle dynamically follows the SC-Trig profile, confirming its practical applicability and ability to mitigate electromagnetic stress during startup transients.
The key numerical findings include: Acceleration performance: Motor speed increases from 0 to 1420 rpm within 1 s, with peak acceleration ≈ 150 rad/s² and zero boundary jerk. Speed tracking accuracy: Velocity error remains below **0.1**%, with no overshoot or oscillations. Torque smoothness: Electromagnetic torque follows a sinusoidal envelope, with no measurable ripple.

Control signal quality: Six-phase PWM signals are stable at 1 kHz, with smoothly varying duty cycle, thus reducing switching stress and protecting power components. These results establish SC-Trig as a superior trajectory planning method, outperforming both polynomial-based approaches and conventional soft-starters in terms of dynamic smoothness, mechanical reliability, and embedded system feasibility. This opens practical opportunities for implementation in industrial applications such as elevators, cranes, and conveyor systems.

4. CONCLUSION

This paper presents a hybrid motor control strategy that combines Field-Oriented Control (FOC) with a trigonometric S-curve (SC-Trig) acceleration profile to improve the startup performance of three-phase induction motors. The proposed method offers second-order continuity in acceleration and jerk, which is a significant improvement over conventional cubic and quintic polynomial profiles that exhibit abrupt transitions or incomplete jerk suppression.

Key quantitative results confirm the effectiveness and novelty of the proposed method: Acceleration time: The motor smoothly reaches 1420 rpm within 1 second, with maximum acceleration ≈ 150 rad/s² and zero boundary jerk. Velocity tracking error: Less than 0.1%, with no overshoot or delay observed between reference and actual speed. Torque response: Electromagnetic torque follows a smooth sinusoidal pattern without measurable ripple, reducing mechanical stress. Control signal quality: Six-phase-shifted PWM signals (U, V, W and complements) are generated at 1 kHz, with duty cycles modulated according to the SC-Trig profile, ensuring stable and continuous operation suitable for industrial drives.

Compared to traditional methods such as linear ramp soft-starters, ANN-based controllers, or start-up frequency tuning, the SC-Trig approach provides better dynamic smoothness, mechanical protection, and real-time implementability on FPGA hardware, as verified in the experimental setup using a DE1-SoC board.

In addition, this research bridges the gap between theoretical motion trajectory design and practical embedded control systems by implementing a complete Verilog-based real-time PWM generator. The outcome confirms the method's applicability in elevators, cranes, and intelligent conveyor systems.

Future research will focus on two directions: (1) Closed-loop experimental validation using actual motor-inverter connections to evaluate robustness under load variations and disturbances; (2) Extension to multi-axis coordinated control systems such as robotic arms or CNC machines, where synchronization and smooth motion are critical.

ACKNOWLEDGMENTS

Research conducted at the Laboratory of Electric Drive Networks and Power Electronics, Room 314, Building A7, Quy Nhon University.

REFERENCES

[1] H.-G. Herzog, Mirza Abdul Waris Begh, "Comparison of Field Oriented Controland Direct Torque Control," *Techrxiv*. March 2018, pp. 1–16, 2018, doi: 10.36227/techrxiv.171332371.13141782/v1.

[2] Lê Thị Thu Phương, Lê Thị Thu Huyền, Phạm Thị Hồng Anh, "Ứng dụng điều khiển vector tựa từ thông rotor cho động cơ không đồng bộ," *Tạp chí khoa học và Công nghệ*, vol. 172, no. 1, pp. 115–119, 2017.

[3] L. T. H. Bui Van Vu, Vo Phuong, DO Van Can, "A survey of working models of direct current motor in PWM rectifier – separately excited direct current motor system," *Journal of Science, Quy Nhon University*, vol. 15, no. 5. pp. 75–85, 2021. doi: 10.52111/qnjs.2021.15508.

[4] T. V. T. Đỗ Văn Cần, "Đề xuất điều khiển vị trí giảm nhiễu đa kênh (ADRC) trên FPGA cho hệ truyền đông Servo," *Tạp chí khoa học trường Đại học Quy Nhontrường Đại học Quy Nhơn*, vol. 12, no. 3, pp. 91–102, 2018.

[5] Do Van Can, "Current controller design based on FPGA," *J. Sci. - Quy Nhon Univ.*, vol. 15, no. 1, pp. 71–78, 2020.

[6] K. Sabahi, M. Teshnehlab, and M. A. shoorhedeli, "Recurrent fuzzy neural network by using feedback error learning approaches for LFC in interconnected power system," *Energy Conversion and Management*, vol. 50, no. 4. pp. 938–946, 2009. doi: 10.1016/j.enconman.2008.12.028.

[7] A. Guellal, C. Larbes, D. Bendib, L. Hassaine, and A. Malek, "FPGA based on-line Artificial Neural Network Selective Harmonic Elimination PWM technique," *Int. J. Electr. Power Energy Syst.*, vol. 68, pp. 33–43, 2015, doi: 10.1016/j.ijepes.2014.11.030.

[8] H. Bai, C. Liu, E. Breaz, and F. Gao, "Artificial neural network aided real-time simulation of electric traction system," *Energy AI*, vol. 1, Aug. 2020, doi: 10.1016/j.egyai.2020.100010.

[9] N. C. N. Dao Huynh Dang Khoa, Su Hong Thanh, "Intelligent control of induction motor using recurrent fuzzy neural networks," *TNU J. Sci. Technol.*, vol. 227, no. 08, pp. 46–55, 2022.

[10] B. Kumar, P. Wang, and A. S. Hossain, "Design of Motion Profile of Stepper Motor for Elevator Using Arduino Uno," *North Am. Acad. Res. J.*, vol. 3, no. 04, pp. 683–695, 2020, [Online]. Available: https://doi.org/10.5281/zenodo.3764537

[11] A. Drumea, C. I. Marghescu, M. P. Ă, G. Jitianu, and A. Vlad, "S-curve motion control implementation using 32-bit microcontroller," in *Proceedings of 2022 International Conference on Hydraulics and Pneumatics - HERVEX November 9-10, Băile Govora, Romania*, 2022, pp. 160–165.

[12] Z. Zhang and Y. Yu, "S-type speed control curve based on the number of pulses," *J. Phys. Conf. Ser.*, vol. 2196, no. 1, 2022, doi: 10.1088/1742-6596/2196/1/012038.

[13] V. Kombarov, V. Sorokin, O. Fojtů, Y. Aksonov, and Y. Kryzhyvets, "S-curve algorithm of acceleration/deceleration with smoothly-limited jerk in high-speed equipment control tasks," *MM Sci. J.*, vol. 2019, no. November, pp. 3264–3270, 2019, doi: 10.17973/MMSJ.2019_11_2019080.

[14] C. Li and F. Chen, "Application of S-curve Acceleration and Deceleration in Winding of Bond-Wire," *Int. J. Trend Res. Dev.*, vol. 8, no. 4, pp. 158–161, 2021.

[15] M. A. Fayrouz Allam, Zaki Nossair, Hesham Gomma, Ibrahim Ibrahim, "Evaluation of Using a Recurrent Neural

Network (RNN) and a Fuzzy Logic Controller (FLC) In Closed Loop System to Regulate Blood Glucose for Type-1 Diabetic Patients," *I.J. Intell. Syst. Appl.*, vol. 10, pp. 58–71, 2012.
[16] Đỗ Văn Cần, "Nghiên cứu thiết kế bộ điều khiển cho hệ truyền động Servo," *Tạp chí Khoa học Trường Đại học Cần Thơ*, vol. 2, no. X, 2016.
[17] X. Li, "Optimizing S-curve Velocity for Motion Control," *J. Appl. Math.*, no. FEBRUARY 2010, pp. 1–12, 2010.
[18] X. Wei, "Acceleration and deceleration control design of step motor based on TMS320F240," *Procedia Eng. Elsevier*, vol. 15, pp. 501–504, 2011, doi: 10.1016/j.proeng.2011.08.095.
[19] V. I. Vlachou, D. E. Efstathiou, and T. S. Karakatsanis, "Design, Analysis and Application of Control Techniques for Driving a Permanent Magnet Synchronous Motor in an Elevator System," *Machines*, vol. 12, no. 8, 2024, doi: 10.3390/machines12080560.
[20] R. Akçelik and M. Besley, "Acceleration and deceleration models," *Springer Ser. Adv. Manuf.*, no. January 2001, pp. 107–156, 2008, doi: 10.1007/978-1-84800-336-1_4.
[21] M. Osama and O. Abdul-Azim, "Implementation and performance analysis of an elevator electric motor drive system," *2008 12th Int. Middle East Power Syst. Conf. MEPCON 2008*, pp. 114–118, 2008, doi: 10.1109/MEPCON.2008.4562368.
[22] G. Cimini, G. Ippoliti, G. Orlando, and M. Pirro, "PMSM control with power factor correction: Rapid prototyping scenario," *Int. Conf. Power Eng. Energy Electr. Drives*, no. May 2013, pp. 688–693, 2013, doi: 10.1109/PowerEng.2013.6635693.
[23] M. Konuhova, "Modeling of Induction Motor Direct Starting with and without Considering Current Displacement in Slot," *Appl. Sci.*, vol. 14, no. 20, 2024, doi: 10.3390/app14209230.
[24] E. S. T. Ralph P. Hervilla, Ruben H. Habaña, Zumel Cadenas, Salem Joh P. Suelon, "Advancements in Three-Phase Electric Motor Control: The Dual Voltag Motor Controller for Seamless Voltage Switching and Enhanced Efficiency," *J. Adv. Zool.*, vol. 44, pp. 1770–1780, 2023.
[25] N. P. Q. Do Van Can, Doan Quang VInh, "Nghiên cứu nâng cao chất lượng gia công máy công cụ nhờ bộ tăng giảm tốc có cấu trúc linh hoạt trên SoCFPGA," in *Cơ kỹ thuật và tự động hoá*, 2016.
[26] K. D. Nguyen, T. C. Ng, and I. M. Chen, "On Algorithms for Planning S-Curve Motion Profiles," *Int. J. Adv. Robot. Syst.*, vol. 5, no. 1, pp. 99–106, 2008, doi: 10.5772/5652.
[27] A. Gavai, A. Kasbekar, and A. V. Mulay, "Position Control of BLDC Motor Using S-Curve for Trajectory Planning and Feedforward Control Design," *2019 10th Int. Conf. Comput. Commun. Netw. Technol. ICCCNT 2019*, no. July 2019, pp. 1–6, 2019, doi: 10.1109/ICCCNT45670.2019.8944914.
[28] A. Gastli and M. M. Ahmed, "ANN-based soft starting of voltage-controlled-fed IM drive system," *IEEE Trans. Energy Convers.*, vol. 20, no. 3, pp. 497–503, 2005, doi: 10.1109/TEC.2004.841522.
[29] R. M. Larik, U. Humayun, and M. Rashid, "Enhancing Three-Phase Induction Motor Performance with Soft Ramp Control," *Int. J. Innov. Sci. Technol.*, no. December, 2024.
[30] A. A. Menaem, S. Beryozkina, and M. Safaraliev, "Intelligent current-speed soft-starting controller for an induction motor drive system," *J. Energy Syst.*, vol. 8, no. 4, pp. 221–236, 2024, doi: 10.30521/jes.1533403.
[31] D. Y. Yang, Y. S. Kim, T. H. Oh, S. H. Lee, and D. Il Cho, "Closed-Loop Soft Starter Firing Angle Control Method Using only Current Feedback," *IEEE Access*, vol. 12, pp. 112062–112073, 2024, doi: 10.1109/ACCESS.2024.3441250.
[32] H. Chen and C. Bi, "Optimal starting frequency of three-phase induction motor," *IET Electr. Power Appl.*, vol. 16, no. 3, pp. 362–369, 2022, doi: 10.1049/elp2.12159.
[33] D. Van Can and T. X. Khoa, "Research design position controller based on FPGA," *Hội nghị - Triển lãm quốc tế lần thứ 7 về Điều khiển và Tự động hoá*, pp. 109–115, 2024.

BIOGRAPHY OF AUTHORS

Do Van Can: https://orcid.org/0009-0000-6599-2221. Born in 1981, received a Master's degree in Automation in 2009 and a Ph.D. degree in 2019 from the University of Danang. Since 2004, he has been a lecturer at the Faculty of Engineering and Technology, Quy Nhon University. His research interests include chip design, FPGA, SoC, electric machine control, CNC machine tools, industrial networks, and SCADA systems. Phone: +84 935 253 630 | Email: dovancan@qnu.edu.vn

Hoang Van Hieu: https://orcid.org/0009-0007-2517-9229. Born in 1983, obtained an engineering degree in Electrical Engineering Technology in 2012. Currently, he is a graduate student (Class K26A) in Electrical Engineering at Quy Nhon University. Since 2012, he has been a lecturer at Kon Tum Vocational School, now known as Kon Tum College. He teaches subjects related to his field of expertise, such as Electric Machines, Electrical Equipment, and Electrical Installation Techniques. Phone: +84 961 164 679 | Email: hieuhoang83vn@gmail.com